Turkish Journal of Electrical Engineering & Computer Sciences

http://journals.tubitak.gov.tr/elektrik/

Research Article

Turk J Elec Eng & Comp Sci
(2018) 26: 125 – 137

doi:10.3906/elk-1704-238

Performance analysis of Hamming code for WSN-based smart grid applications

Melike YİĞİT[1,*], Vehbi Çağrı GÜNGÖR[2], Pınar BÖLÜK[3]

[1]Department of Computer Engineering, Graduate School of Natural and Applied Sciences, Bahçeşehir University, İstanbul, Turkey

[2]Department of Computer Engineering, Faculty of Engineering, Abdullah Gül University, Kayseri, Turkey

[3]Department of Software Engineering, Faculty of Engineering, Bahçeşehir University, İstanbul, Turkey

Received: 20.04.2017 • **Accepted/Published Online:** 15.11.2017 • **Final Version:** 26.01.2018

Abstract: Many methods have been employed to detect, compare, and correct errors to increase communication reliability and efficiency in wireless sensor networks (WSNs). However, to the best of our knowledge, no existing study has compared the performance of error control codes by using different modulation techniques in a smart grid communication environment when multichannel scheduling is used. This paper presents a detailed performance evaluation and makes a comparison of different modulation techniques, such as frequency shift keying (FSK), differential phase shift keying (DPSK), binary phase shift keying (BPSK), and offset quadrature phase-shift keying (OQPSK), using Hamming codes in a 500-kV line-of-sight substation smart grid environment with multichannel scheduling. A link-quality-aware routing algorithm is used as a routing protocol and a log-normal shadowing channel is employed as a channel model. Simulations are performed in MATLAB and the performance of the Hamming code with various modulation techniques is compared with the results obtained without using any error correction codes for throughput, delay, and bit error rate. The results show that the performance of the Hamming code with OQPSK modulation is better than its performance with other modulation techniques. Moreover, the results show that the performance of Hamming code improves with multichannel scheduling for all modulation techniques.

Key words: Hamming code, modulation, multichannel scheduling, smart grid

1. Introduction

Smart grids can be considered as the modern power grids, integrating electrical networks and information technologies. The basic components and technologies of a smart grid can be listed as smart production, smart stations, smart deployment, smart meters, integrated communication, and advanced control methods [1-5]. With these components and technologies, a smart grid provides many benefits, such as demand management, greater integration of renewable resources, efficient usage of renewable resources (on both the production and consumption sides), energy-saving and price advantages, and system balance [1,6-9,10,11] All these benefits can be achieved with a reliable communication infrastructure. Therefore, error detection and correction become critical issues for a wireless sensor network (WSN)-based smart grid communication network. However, providing reliable communication between consumers and utilities in a smart grid communication environment is difficult due to harsh channel conditions such as noise, path loss, fading, and shadowing [1,6,12,13].

Various error detection and correction studies [12,14,15] have been performed for WSNs in the literature.

*Correspondence: melike.yigit@stu.bahcesehir.edu.tr

In [14], the performance of Reed–Solomon (RS) codes using binary phase shift keying (BPSK) modulation was evaluated in an additive white Gaussian noise channel. Bit error rate (BER) was measured while the signal energy-to-noise power density ratio (E_b/N_0) was increasing. The results showed that BER performance increases when code word length remains constant for the same code rate. Furthermore, the results showed that the performance of RS code, which has more parity check bits to correct burst errors, has a higher BER value when E_b/N_0 is low. In [12], RS and Hamming codes were compared. As a result of the comparative analysis, it was found that the performance of RS code is better for data communication than Hamming code, because RS provides a high coding rate with low coding complexity. Moreover, the results of the analysis showed that the Hamming code is efficient for transmitting small data sizes, since it is simple and can correct one error per message. The performance of RS and Bose–Chaudhuri–Hochquenghem (BCH) codes was evaluated in [15] over a correlated Rayleigh fading channel by using a quadrature amplitude modulation (QAM) modulation technique. Various modulation orders of the QAM were used to show how the modulation order affects the performance of RS and BCH codes. BER was used as a performance metric, whereby the BER performance of RS and BCH was measured with different QAM modulation orders as the signal-to-noise ratio (SNR) increased. The simulation results showed that the BER performance of a channel not using coding increases when the SNR and modulation order increase. However, the BER performance of RS and BCH is not as good as the BER performance of a channel without coding when the modulation order increases. In addition, it was shown that the BER performance of BCH 64-QAM was highest among all others, namely BCH 16-QAM, BCH 32-QAM, RS 16-QAM, RS 32-QAM, and RS 64-QAM.

Although there exist a few performance comparisons of error detection and correction codes for WSNs, these studies have not focused on WSN-based smart grid applications and their communication environments. Therefore, in this paper, the performance of the Hamming code with various modulation techniques, such as frequency shift keying (FSK), differential phase shift keying (DPSK), offset quadrature phase-shift keying (OQPSK), and binary phase shift keying (BPSK), is measured in terms of throughput, BER, and delay in a 500-kV LOS substation smart grid environment. Multichannel scheduling and a link-quality-aware routing algorithm (LQ-CMST) are used to transmit data from the sender to the sink node [16]. Therefore, the impact of multiple channels on the performance of the Hamming code, using different modulation techniques, is measured. In addition, the performance evaluation of the Hamming code with OQPSK modulation is conducted with varying packet sizes and output powers to show how these aspects affect the performance of the Hamming code with OQPSK modulation. Furthermore, our objective is to indicate whether or not a modulation technique involving Hamming code should be favored for smart grid communication environments when multichannel scheduling is used.

Overall, the main contribution of this study is investigating the performance of the Hamming code with different modulation techniques, such as FSK, DPSK, OQPSK, and BPSK, and quantifying how multichannel communication combined with the LQ-CMST routing protocol will affect the performance of Hamming code in terms of throughput, BER, and delay under the harsh conditions of a 500-kV LOS substation smart grid environment.

The remainder of this paper is organized as follows. In Section 2, Hamming code is described in detail. In Section 3, materials and methods are explained. Performance analysis and simulation results are presented in Section 4. The discussion of the simulation results is presented in Section 5. Finally, the paper is concluded with a consideration of future work in Section 6.

$$Code\ word\ length:\ n = 2^m - 1,\ \text{for}\ m \geq 2 \tag{1}$$

$$\#\ of\ information\ bits:\ k = 2^m - m - 1 \tag{2}$$

$$\#\ of\ parity\ bits: n - k = m \tag{3}$$

$$\#\ of\ error\ correction\ bits:\ t = 1 \tag{4}$$

2. Hamming code

Hamming code was the first forward error correction (FEC) coding technique, invented by Richard Hamming in 1940 [12]. FEC is an error control technique used to transmit data through unreliable communication channels. The main purpose of FEC is to encode messages by using an error correction code (ECC). FEC coding techniques are classified as block and convolutional codes [17,18]. The Hamming coding system is a kind of binary block code method used in telecommunications [19]. With the Hamming coding method, single-bit errors in a data packet can be found and corrected. Additionally, three-bit errors are detected using this method; however, these errors cannot be corrected. Hamming codes are expressed as shown in Eqs. (1)–(4).

$$d_1 = \begin{bmatrix} 1 \\ 0 \\ 0 \\ 0 \end{bmatrix}, \quad d_2 = \begin{bmatrix} 0 \\ 1 \\ 0 \\ 0 \end{bmatrix}, \quad d_3 = \begin{bmatrix} 0 \\ 0 \\ 1 \\ 0 \end{bmatrix}, \quad d_4 = \begin{bmatrix} 0 \\ 0 \\ 0 \\ 1 \end{bmatrix} \tag{5}$$

$$P_1 = d_2 + d_3 + d_4, \text{ where } P_1 = \begin{bmatrix} 0 \\ 1 \\ 1 \\ 1 \end{bmatrix} \tag{6}$$

$$P_2 = d_1 + d_3 + d_4, \text{ where } P_2 = \begin{bmatrix} 1 \\ 0 \\ 1 \\ 1 \end{bmatrix} \tag{7}$$

$$P_3 = d_1 + d_2 + d_4, \text{ where } P_3 \begin{bmatrix} 1 \\ 1 \\ 0 \\ 1 \end{bmatrix} \tag{8}$$

2.1. Hamming encoder

A Hamming encoder block encodes the information bits before transmission through the channel. In this study, Hamming (7, 4) code is used. This means that the code word length is 7 (n = 7) and the size of information bits and parity check bits is 4 (k = 4) and 3 (m = 3), respectively. First the information bits (I_1, I_2, I_3, I_4) of length k bits are encoded by adding three parity bits (P_1, P_2, P_3) to form the code word (C) over the elements

of a Galois finite field (GF) (2^m). Next, d matrices, which are k $\times$ 1 column vectors, as shown in Eq. (5), are used to form the parity matrices [20-22]. As shown in Eqs. (6)–(8), parity matrices (P_1, P_2, P_3) are formed by adding d matrices.

Information and parity bits can be mixed together in different ways [23]. In this paper, parity bits are put at the beginning of information bits. Hamming codes are linear block codes. Therefore, two matrices, parity-check matrix H and generator matrix G, are used. The information bits (I) are multiplied by the G matrix to obtain the code word (C). In Eq. (9), the encoding equation and G matrix used in this study are shown.

$$C = I \times G, \text{ where } G = \begin{bmatrix} 0 & 1 & 1 & 1 & 0 & 0 \\ 1 & 0 & 1 & 0 & 1 & 0 \\ 1 & 1 & 0 & 0 & 0 & 1 \\ 1 & 1 & 1 & 0 & 0 & 0 \end{bmatrix} \tag{9}$$

2.2. Hamming decoder

A parity check matrix is used in the decoding process. The parity check matrix used in this study is shown in Eq. (10). The received code word (C) of 7 bits (information bits (K) + parity bits (H)) is multiplied by the transpose of the parity check matrix H, as shown in Eq. (11), to obtain the syndrome vector (S). This shows whether or not an error occurs. If an error occurs [24,25], it indicates that there is an error for a particular code word bit. If all the bits of the syndrome vector are zero, this means that the data have not been corrupted during transmission. However, if one of the data bits is corrupted due to bad channel conditions, such as a noisy channel, the syndrome vector shows the place of the error in the code word bit. For instance, if the code word C = 1011010 is received without any errors, the syndrome matrix will become S = (0, 0, 0). However, if the code word is received with an error, such as C = 1011011, the syndrome matrix will become S = (1, 1, 1). This means that the 7th bit of the code word is corrupted. If the 7th bit of the corrupted code word is 1, it is changed to 0 and the corrected code word is obtained. The last four bits are the original information bits and the first three bits are ignored.

$$H = \begin{bmatrix} 1 & 0 & 0 & 0 & 1 & 1 & 1 \\ 0 & 1 & 0 & 1 & 0 & 1 & 1 \\ 0 & 0 & 1 & 1 & 1 & 0 & 1 \end{bmatrix} \tag{10}$$

$$S = C \times H^T, \text{ where } H^T = \begin{bmatrix} 1 & 0 & 0 \\ 0 & 1 & 0 \\ 0 & 0 & 1 \\ 0 & 1 & 1 \\ 1 & 0 & 1 \\ 1 & 1 & 0 \\ 1 & 1 & 1 \end{bmatrix} \tag{11}$$

3. Materials and methods

3.1. System model

K number of information bits (I) is given as an input to the Hamming encoder. The Hamming encoder encodes these bits, as described in Section 2.2, to obtain the code word (C). The code word is passed to the digital modulator, which uses one of the modulation schemes, such as FSK, BPSK, OQPSK, and DPSK, to transform the information bits into digital waveforms. After the modulation, the information bits are sent through the log-normal shadowing channel, which incorporates harsh channel conditions such as noise, scattering, reflection, and diffraction. These channel conditions can affect and corrupt the code word. After the transmission of the code word over the channel finishes, it is demodulated with the demodulator using one of the FSK, BPSK, OQPSK, or DPSK demodulation schemes. The demodulated code word (C') is then sent to the Hamming decoder to decode the code word into the original information bits (I'). Decoded information bits (I') are controlled, and if there is no error, it is received by the sink node. The block diagram of this system model is shown in Figure 1.

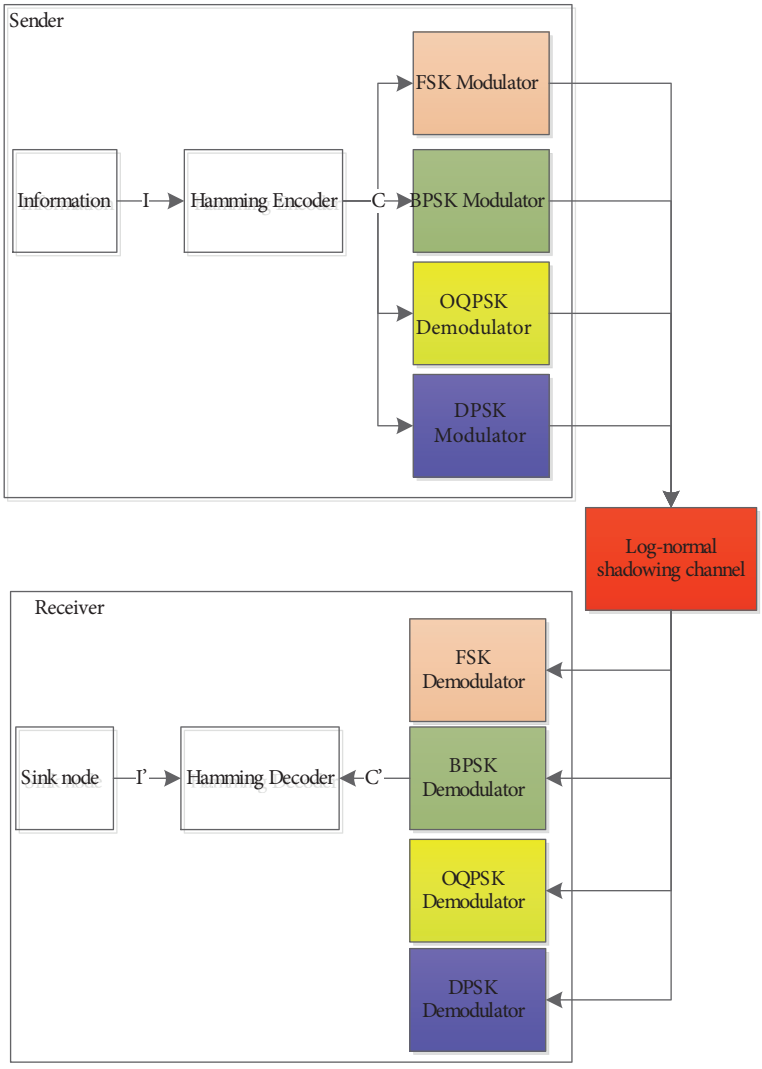

Figure 1. Block diagram of the system model.

3.2. Protocol description

In this study, we modeled a WSN model composed of source nodes, relay nodes, and a sink node. Additionally, we constructed a graph G = (V, E) for this WSN model; the set of vertexes of this graph is shown as V, which represents the set of nodes. The set of edges of this graph is shown as E, which represents the wireless links. We used half-duplex data transmission, which means that data communication can be performed in two directions: from sender to receiver and vice versa, but not at the same time. A receiver-based channel assignment (RBCA) algorithm, which is a multichannel medium access control (MAC) protocol, is used, together with the LQ-CMST routing protocol. The LQ-CMST proposed in [16] is a routing protocol that considers link qualities (packet reception rate (PRR)) while constructing a routing tree. The RBCA proposed in [26] assigns the channels statically to the receivers by considering the interference experienced by them [27]. After assigning the channels, the RBCA makes a time slot assignment by using a time division multiple access (TDMA) protocol for parallel transmission scheduling, also known as multichannel scheduling, through the multiple branches of the LQ-CMST routing tree.

3.3. Channel and PRR models

A log normal shadowing channel model, which is a radio propagation model that measures the path loss that occurs due to distance and obstructions, is used. The 500-kV LOS substation smart grid environment path loss (γ) and shadowing deviation (X_σ) parameters, shown in Table 1, are used to calculate the log-normal path loss equation and are explained in Eq. (12) [27]:

Table 1. Path loss and shadowing deviation parameters of 500-kV substation (LOS) smart grid environment.

Path loss (γ)	2.42
Shadowing deviation (σ)	3.12

$$\lambda(d) = P_{T_x} - P_{R_x} = PL_0 + 10 \times \lambda \times \log_{10} \frac{d}{d_0} + X_\sigma \tag{12}$$

where γ(d) is the path loss measured in decibels (dB), and P_{Tx} and P_{Rx} are the transmitted power and the received power in dBm, respectively. PL_0 is the path loss at distance d_0; d and d_0 are path length and reference distance, respectively; γ is the path loss exponent; and $X\sigma$ is the Gaussian random variable with zero mean.

4. Performance analysis

In this section, the performance of the Hamming code, integrated with the different modulation schemes, is evaluated using multichannel scheduling. Furthermore, the results of the Hamming code are compared with the results obtained without using error control codes.

4.1. Simulation parameters

The LQ-CMST routing protocol, multichannel scheduling algorithm, and Hamming code were implemented in MATLAB and extensive simulations were conducted with a MATLAB simulation tool. The simulation parameters are shown in Table 2. A realistic channel model was used by utilizing a log-normal shadowing model, as explained in Section 3.3.

Table 2. Simulation parameters.

Parameters	Values
Modulation schemes	BPSK, DPSK, OQPSK, FSK
Output power	4 dB
Noise floor	–93 dB
Number of nodes	120
Size of topology	200 × 200 m^2
Encoding	Manchester

In the performance evaluations, 120 nodes are used. These nodes are randomly deployed over a 200 × 200 m^2 area. For each simulation, we run the experiments 100 times, and an average of the measured results is taken. We assume that each node generates one packet at the beginning of scheduling. Packets generated by the source nodes are forwarded through multiple hops to the sink node. A best-effort delivery model with multichannel scheduling is assumed. Therefore, no retransmission is performed if the packet is lost.

4.2. Simulation results

The performance of the Hamming code, integrated with different modulation schemes such as BPSK, DPSK, FSK, and OQPSK, is evaluated and compared with the results obtained without using an error correction code in a 500-kV LOS substation smart grid environment. Throughput, delay, and BER are used as performance metrics. Simulations are performed to show how the modulation and number of channels affect the throughput, delay, and BER performance of the Hamming code. Then the impact of packet size and output power on the throughput, delay, and BER performance of Hamming code, combined with OQPSK modulation, was addressed in a smart grid environment.

Figures 2 and 3 show the throughput and delay performance of the Hamming code, respectively, without ECC with varying modulation schemes such as BPSK, DPSK, FSK, and OQPSK when the number of channels increases. The results show that the throughput of the network increases and the delay of the network decreases with all of the Hamming code, and without ECC combined with different modulation schemes, when the number of channels increases, as shown in Figures 2 and 3. This is because multiple channels minimize interference to avoid packet loss and provide simultaneous transmission to increase the number of packets transmitted to the sink node in a shorter period of time. Figures 2 shows that the throughput performance of the Hamming code is better than that without ECC. In addition, in Figure 2, it is observed that the Hamming code with OQPSK modulation shows the best performance in terms of throughput using 16 channels. Figure 3 shows that the delay performance of the Hamming code is worse than that without ECC. Furthermore, in Figure 3, it is shown that without ECC with OQPSK, the modulation shows the best performance in terms of delay when the number of channels is 16.

In Figure 4, the BER performance of the Hamming code and without ECC is compared in terms of different modulation schemes and a varying number of channels. It can be seen from this figure that when the number of channels increases, BER decreases for all cases, such as Hamming code and without ECC combined with different modulation schemes, since the impact of interference is eliminated by multichannel scheduling. Figure 4a shows the BER performance of the Hamming code and without ECC with the BPSK modulation. The results show that the Hamming code performs better with BER values of 10^{-6}, 10^{-9}, and 10^{-12} for 1, 8, and 16 channels, respectively, than the BER performance without ECC. Figure 4b shows the BER results of

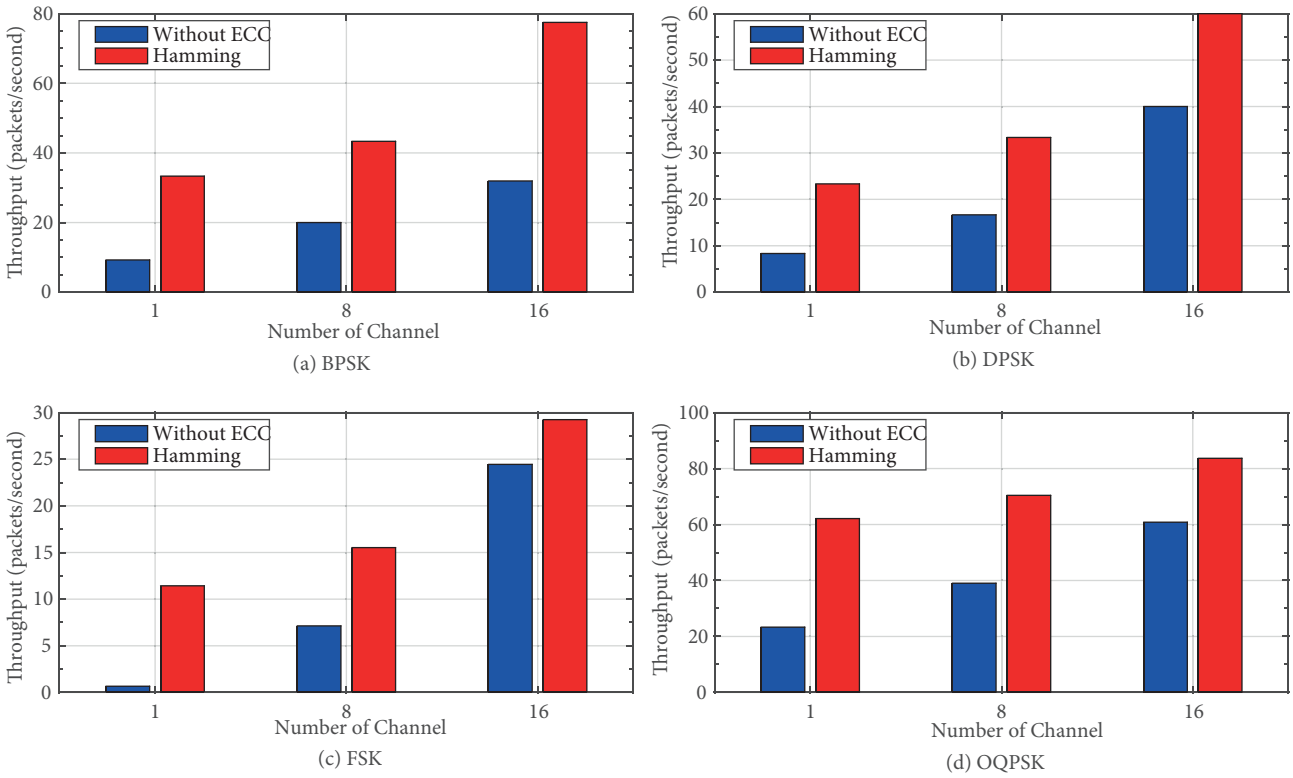

Figure 2. Throughput vs. number of channel for log-normal shadowing channel (using BPSK, DPSK, FSK, and OQPSK) without ECC and Hamming code in a 500-kV LOS substation smart grid environment.

the Hamming code and without ECC, integrated with the DPSK modulation scheme. The graph shows that Hamming-coded DPSK performs better with BER values of 10^{-6}, 10^{-8}, and 10^{-9} for 1, 8, and 16 channels than the BER performance without ECC. Figure 4c shows the BER values of the Hamming code without ECC when FSK is used as the modulation scheme. It can be seen from the figure that Hamming-coded FSK has smaller BER values, i.e. 10^{-4}, 10^{-6}, and 10^{-8}, than the BER values without ECC. The BER performance of the Hamming code without ECC and with OQPSK modulation is shown in Figure 4d. The results obtained show that the Hamming code with OQPSK modulation has the lowest BER values of 10^{-8}, 10^{-10}, and 10^{-13} at channels 1, 8, and 16, respectively. As a result, it is observed that the Hamming code with OQPSK modulation shows the best performance in terms of BER with 16 channels.

The simulation results show that the Hamming code combined with OQPSK modulation provides the best results for a 500-kV LOS substation smart grid environment. For this reason, the performance of the Hamming code combined with OQPSK modulation is evaluated for various output powers and packet sizes in Figures 5 and 6, respectively. Figures 5a and 5b show the BER and delay in terms of the performance of the Hamming code with OQPSK modulation for variable output powers and number of channels. These figures show that BER and delay slowly decrease when the output power is more than 4 dBm. Furthermore, the minimum BER and delay results are obtained when the number of channels is 16. Figure 5c shows the throughput results of the Hamming code with OQPSK modulation for different output powers. The results show that throughput slowly increases when the output power increases. In addition, the results present that the highest throughput is achieved when the number of channels is 16. Figures 6a and 6b show BER and the delay results of the

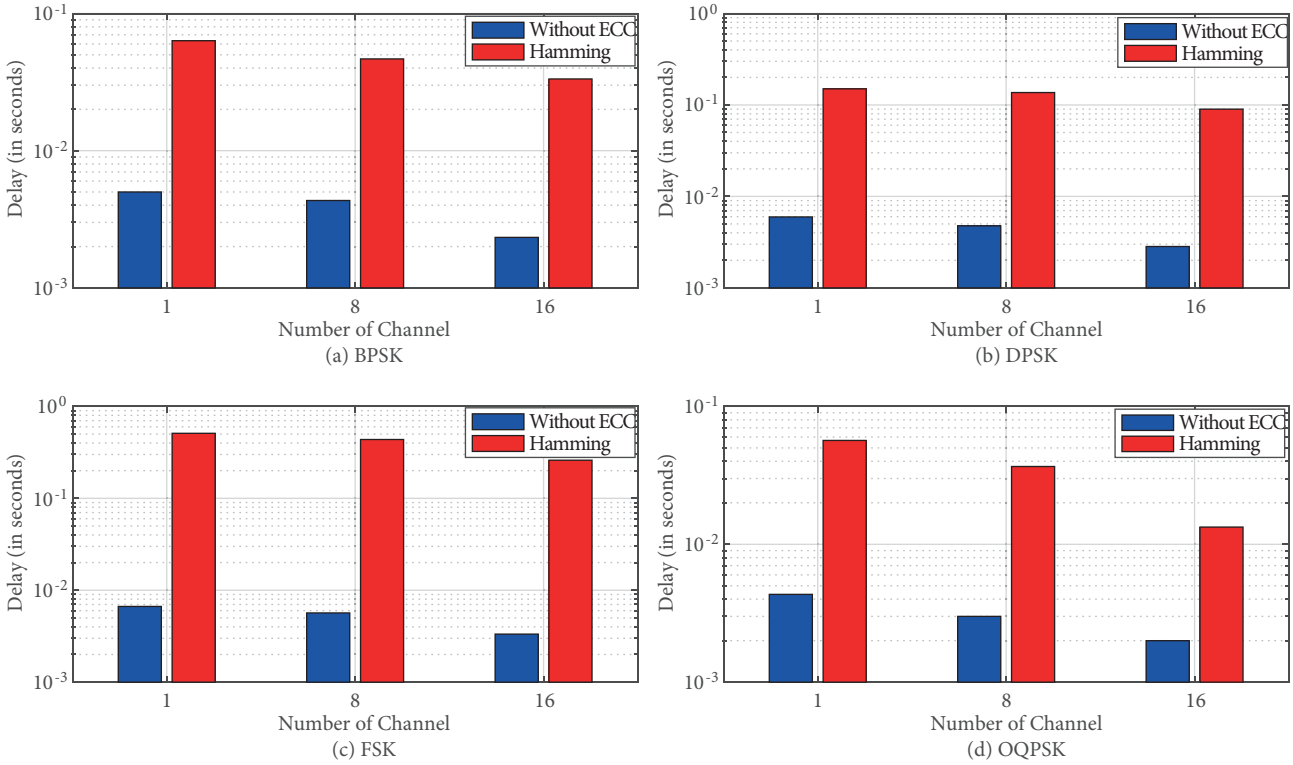

Figure 3. Delay vs. number of channel for log-normal shadowing channel (using BPSK, DPSK, FSK, and OQPSK) without ECC and Hamming code in a 500-kV LOS substation smart grid environment.

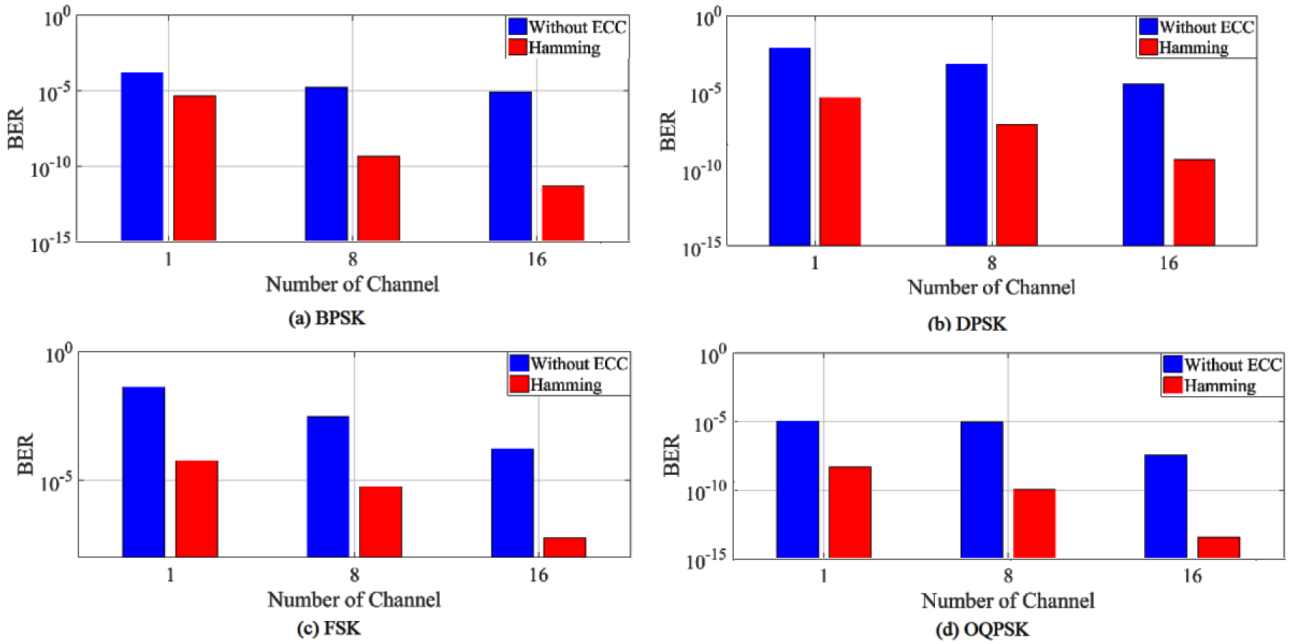

Figure 4. BER vs. number of channel for log-normal shadowing channel (using BPSK, DPSK, FSK, and OQPSK) without ECC and Hamming code in a 500-kV LOS substation smart grid environment.

Hamming code with OQPSK modulation for a variable number of channels and packet sizes. These results show that BER and delay increase as the packet size increases; similarly, the best BER and delay results are obtained when the number of channels increases to 16. Furthermore, it is observed that delay sharply increases when the packet size is bigger than 180 bytes. This situation affects the throughput results, as throughput and delay are directly proportional to each other. As shown in Figure 6c, throughput sharply decreases when the packet size is larger than 180 bytes. In addition, Figure 6c shows that throughput increases until the packet size reaches 100 bytes and slowly decreases when the packet size is between 100 and 180 bytes.

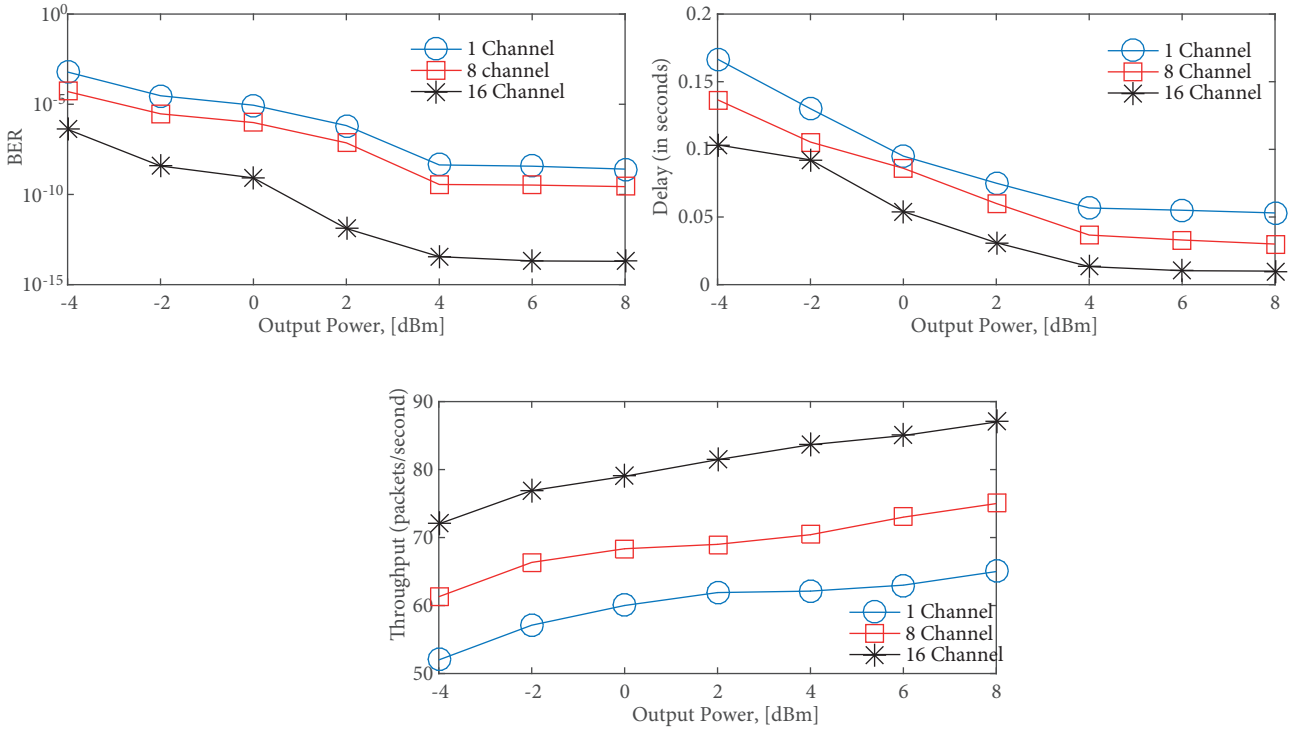

Figure 5. Throughput, BER, and delay vs. output power for log-normal shadowing channel using OQPSK with Hamming code by increasing the number of channels in 500-kV LOS substation smart grid environment.

The performance results clearly show that using an error correction code, such as the Hamming code, increases performance in terms of BER, throughput, and delay in a 500-kV LOS substation smart grid environment. In addition, the choice of modulation scheme considerably affects the performance of a smart grid communication system.

5. Discussion

Examining the simulation results, we found that the Hamming code performed well only for applications that require low BER and high throughput. It minimizes BER and maximizes the number of received packets compared to without ECC; however, it increases delay. This is because it adds parity bits to correct the error, which causes extra overhead. Furthermore, Hamming encoding and decoding cause additional communication delays. Performance results show that the modulation scheme significantly affects the performance of the Hamming code and without ECC. There are other studies [28-30] that showed the impact of the modulation scheme on the communication quality in different network systems. According to these studies, the OQPSK modulation scheme outperforms the other schemes, similarly to our study. This is because OQPSK provides a

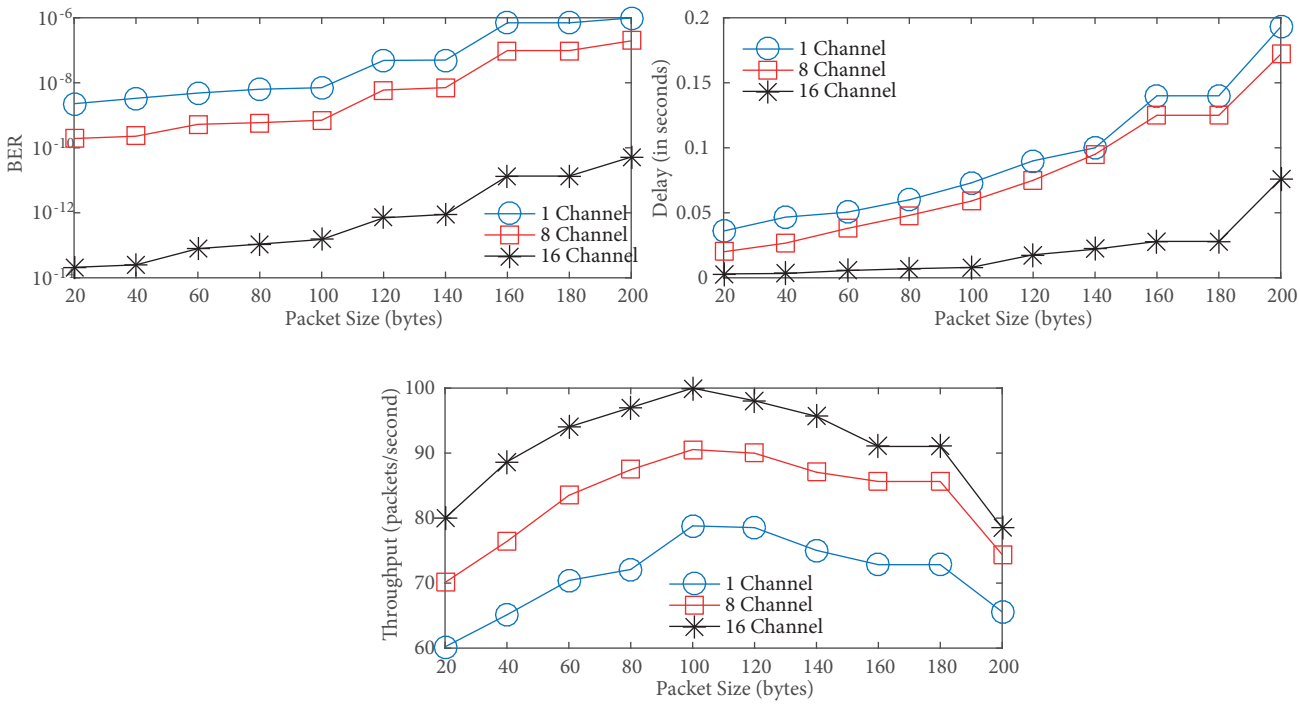

Figure 6. Throughput, BER, and delay vs. packet size for log-normal shadowing channel using OQPSK with Hamming code by increasing the number of channels in a 500-kV LOS substation smart grid environment.

higher data rate compared to BPSK, DPSK, and FSK. For the same bit error rate, the required bandwidth by OQPSK is less than the other modulation schemes.

The impact of multichannel scheduling and LQ-CMST routing on the performance of the Hamming code have been evaluated. All the results show that network performance improves when multichannel scheduling is used, since multichannel communication minimizes the impact of interference by achieving simultaneous transmission over multiple channels.

The performance of the Hamming code combined with OQPSK modulation has been evaluated for different packet sizes and various output powers for WSNs in a 500-kV LOS substation smart grid environment. We have observed that when the output power increases, the performance of the Hamming code improves. This is because high output power increases the reliability of the network by decreasing the number of packet losses, as expected. On the other hand, the same result cannot be obtained by increasing the packet size. High packet size adversely affects the delay and BER performance of the Hamming code combined with OQPSK modulation. Therefore, although throughput increases until the packet size reaches 100 bytes, packet size must be chosen carefully according to application requirements in the 500-kV LOS substation smart grid environment.

6. Conclusion

This paper presented the performance of the Hamming code combined with different modulation schemes such as BPSK, DPSK, FSK, and OQPSK in a 500-kV LOS substation smart grid environment. Simulations were performed to evaluate the impact on the number of channels, variable packet size, and output power on BER, delay, and throughput in a 500-kV LOS substation smart grid environment. Comparative performance evaluations were presented to show the extent of BER, delay, and throughput change when different modulation schemes and a variable number of channels are used. The simulation results show that the performance of

the Hamming code with OQPSK modulation is better than its performance with other modulation schemes. Additionally, the results indicate that multichannel scheduling significantly improves network performance, as the best results are obtained when the number of channels is 16.

Overall, our main contribution has been investigating the performance of the Hamming code with different modulation schemes in a 500-kV LOS substation smart grid environment and measuring the impact of multichannel scheduling on the performance of the Hamming code. To the best of our knowledge, no existing study has evaluated the performance of the Hamming code with different modulation schemes and with a varying number of channels in a 500-kV LOS substation smart grid environment. Hence, this study will provide valuable insights into the development of error correction codes combined with different modulation schemes in a smart grid environment. For future work, we plan to investigate the performance of other error correction codes and routing algorithms in different smart grid environments, such as main power control rooms and underground transformer vaults.

Acknowledgments

The work of VÇ Güngör was supported by the Abdullah Gül University Foundation and the Turkish National Academy of Sciences Distinguished Young Scientist Award Program (TÜBA-GEBİP) (Grant No. V.G./TBA-GEBP/2013-14).

References

[1] Gungor VC, Lu B, Hancke GP. Opportunities and challenges of wireless sensor networks in smart grid. IEEE T Ind Electron 2010; 57: 3557-3564.

[2] Gungor VC, Sahin D, Kocak T, Ergut S, Buccella C, Cecati C, Hancke GP. A survey on smart grid potential applications and communication requirements. IEEE T Ind Inform 2013; 9: 28-42.

[3] Fadel E, Gungor VC, Nassef L, Akkari N, Malik MA, Almasri S, Akyildiz IF. A survey on wireless sensor networks for smart grid. Comput Commun 2015; 71: 22-33.

[4] Yan Y, Qian Y, Sharif H, Tipper D. A survey on smart grid communication infrastructures: motivations, requirements and challenges. IEEE Commun Surv Tut 2013; 15: 5-20.

[5] Fan Z, Kulkarni P, Gormus S, Efthymiou C, Kalogridis G, Sooriyabandara M, Chin WH. Smart grid communications: overview of research challenges, solutions, and standardization activities. IEEE Commun Surv Tut 2013; 15: 21-38.

[6] Gungor VC, Sahin D, Kocak T, Ergut S, Buccella C, Cecati C, Hancke GP. Smart grid technologies: communication technologies and standards. IEEE T Ind Inform 2011; 7: 529-539.

[7] Fang X, Misra S, Xue, G, Yang D. Smart grid: the new and improved power grid: a survey. IEEE Commun Surv Tut 2012; 14: 944-980.

[8] Depuru SSSR, Wang L, Devabhaktuni V. Smart meters for power grid: challenges, issues, advantages and status. Renew Sust Energ Rev 2011; 15: 2736-2742.

[9] Turan M, Erdin G. Relay coordination analysis and protection solutions for smart grid distribution systems. Turk J Elec Eng & Comp Sci 2016; 24: 474-482.

[10] Janjic A, Savic S, Velimirovic L, Nikolic V. Renewable energy integration in smart grids-multicriteria assessment using the fuzzy analytical hierarchy process. Turk J Elec Eng & Comp Sci 2015; 23: 1896-1912.

[11] Bjelica M, Pejovic MS. Communications protocol for power management in smart homes. Turk J Elec Eng & Comp Sci 2017; 25: 1554-1562.

[12] Okeke C, Eng M. A comparative study between hamming code and Reed-Solomon code in byte error detection and correction. Int J Res Appl Sci 2015; 3: 34-39.

[13] Usman A, Shami SH. Evolution of communication technologies for smart grid applications. Renew Sust Energ Rev 2013; 19: 191-199.

[14] Korrapati V, Prasad MVD, Reddy DV, Tej GA. A study on performance evaluation of Reed Solomon codes through an AWGN channel model for an efficient communication system. Int J Eng Trends 2013; 4: 1038-1041.

[15] Akande DO, Ojo FK, Abolade RO. Performance of RS and BCH codes over correlated Rayleigh fading channel using QAM modulation technique. J Inform Eng Appl 2014; 4: 88-94.

[16] Yigit M, Gungor VC, Fadel E, Nassef L, Akkari N, Akyildiz IF. Channel-aware routing and priority-aware multi-channel scheduling for WSN-based smart grid applications. J Netw Comput Appl 2016; 71: 50-58.

[17] Vuran MC, Akyildiz IF. Error control in wireless sensor networks: a cross layer analysis. IEEE ACM T Netw 2009; 17: 1186-1199.

[18] Manzoor B, Javaid N, Rehman O, Bouk SH, Ahmed SH, Park SH, Kim D. Energy aware error control in cooperative communication in wireless sensor networks. ACM SIGAPP Appl Comput Rev 2014; 14: 55-64.

[19] Wicker SB. Error Control Systems for Digital Communication and Storage. Vol. 1. Upper Saddle River, NJ, USA: Prentice Hall, 1995.

[20] Malode MV, Patil DB. PAPR reduction using modified selective mapping technique. Int J Adv Netw Appl 2010; 2: 626-630.

[21] Fu B, Ampadu P. On hamming product codes with type-II hybrid ARQ for on-chip interconnects. IEEE T Circuits-I 2009; 56: 2042-2054.

[22] Moon TK. Error Correction Coding: Mathematical Methods and Algorithms for Signal Processing. Hoboken, NJ, USA: Wiley, 2005.

[23] Mstafa RJ, Elleithy KM. A highly secure video steganography using Hamming code (7, 4). In: IEEE 2014 Long Island Systems, Applications and Technology Conference; 1–6 May 2014; Farmingdale, NY, USA. New York, NY, USA: IEEE. pp. 1-6.

[24] Hamming RW. Coding and Theory. Upper Saddle River, NJ, USA: Prentice Hall, 1980.

[25] Howard SL, Schlegel C, Iniewski K. Error control coding in low-power wireless sensor networks: when is ECC energy-efficient? EURASIP J Wirel Comm 2006; 2: 29-29.

[26] Incel OD, Ghosh A, Krishnamachari B, Chintalapudi K. Fast data collection in tree-based wireless sensor networks. IEEE T Mobile Comput 2012; 11: 86-99.

[27] Yigit M, Incel OD, Gungor VC. On the interdependency between multi-channel scheduling and tree-based routing for WSNs in smart grid environments. Comput Netw 2014; 65: 1-20.

[28] El-Nahal FI, Salha MA. Comparison between OQPSK and DPSK bidirectional radio over fiber transmission systems. Universal Journal of Electrical and Electronic Engineering 2013; 1: 129-133.

[29] Kumar S, Sharma S. Error probability of different modulation schemes for OFDM based WLAN standard IEEE 802.11 a. Int J Eng 2010; 4: 262-267.

[30] Panicker NV, Sukesh AK. BER performance evaluation of different digital modulation schemes for biomedical signal transceivers under AWGN and fading channel conditions. Int J Eng Adv Technol 2014; 4: 212-215.